JOURNAL OF MATERIALS SCIENCE 15 (1980) 563–574

Further refinements in the energy of grain boundaries

K. JAGANNADHAM, M. J. MARCINKOWSKI
Department of Mechanical Engineering and Engineering Materials Group, University of Maryland, College Park, Maryland 20742, USA

Earlier surface dislocation analysis of a grain boundary recognized the tendency of the grain-boundary surfaces to coalesce in order to reduce surface energy. The coalescence process is described by a distribution of surface dislocations on the grain-boundary surfaces. In the present paper, previous analysis is further refined. In particular, the sum of the Burgers vectors of the surface array of grain-boundary dislocations is not equal to the Burgers vector of the grain-boundary lattice dislocation. Instead, the Burgers vector of the surface array is determined as a function of the coalescence of the grain-boundary surfaces. The conservation of Burgers vectors of dislocations is used to predict the presence of a screening array of dislocations. The screening array of dislocations is determined by minimization of the total energy of the configuration. The distortion around the boundary is relaxed by the screening array. In general, the distribution of the screening array is two dimensional. This result has been proved by the presence of a minimum energy configuration for two sets of screening arrays of dislocations situated at different distances from the boundary.

1. Introduction

Earlier geometric models of grain boundaries [1–5] related the grain-boundary misorientation angle to the spacing between dislocations in the boundary and the Burgers vector. One of the chief drawbacks of the geometric models has been pointed out as the inability to describe the atomic relaxation at the grain boundary so that the energy of the grain boundary cannot also be determined. This limitation of the geometric models is overcome by the surface dislocation analysis of the grain boundary [6–8]. In the unified theory of grain boundaries, the grain-boundary dislocations representing the ledge steps, as shown in Fig. 1a are formed by gliding a crystal lattice dislocation from the two adjacent grains [1–4]. Fig. 1a is a completely torn or relaxed state of the grain boundary [9]. The grain boundary has no stresses associated with it since there are no elastic dislocations. Therefore, it follows that the grain-boundary dislocations have no stress associated with them but the ledge steps do provide a surface contribution. In the previous surface dislocation model of the grain boundary [6–8], the coalescence of the grain-boundary surfaces to reduce the surface energy has been recognized, as shown in Fig. 1b. The coalescence of the grain-boundary surfaces is explained by distributing surface dislocations on the grain-boundary surfaces. The fully coalesced grain boundary, which is a hypothetical situation, is shown in Fig. 1c where the grain-boundary surfaces coalesced completely and eliminated the surface. The surface dislocation array on the grain-boundary surfaces has been chosen in the earlier models with Burgers vector equal to the Burgers vector of the grain-boundary lattice dislocations. However, further considerations of the coalescence of the grain-boundary surfaces has shown that the total Burgers vector of the surface array on the grain-boundary surfaces is less than the sum of the Burgers vector of the grain-boundary lattice dislocations. The refined analysis, taking into account that the grain-boundary surface array has a Burgers vector which is a function of the degree of coalescence of the grain-boundary surfaces will be presented in this paper.

0022-2461/80/030563–12$03.20/0

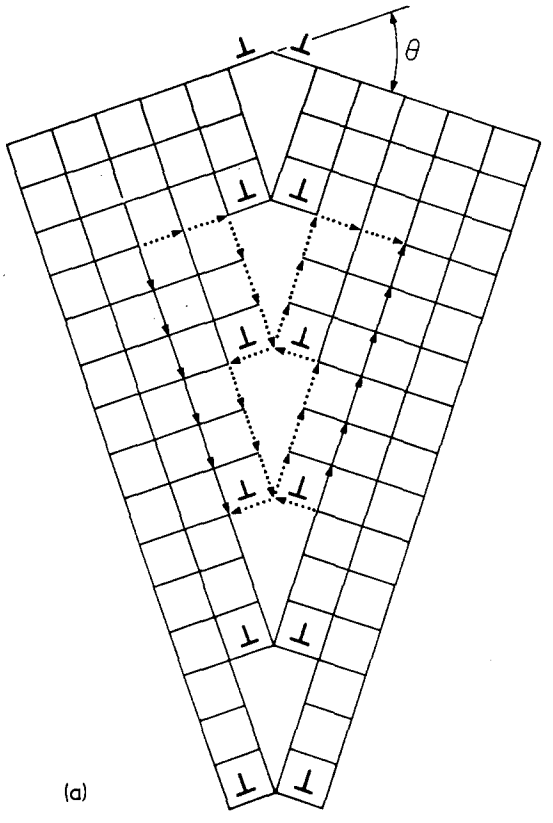

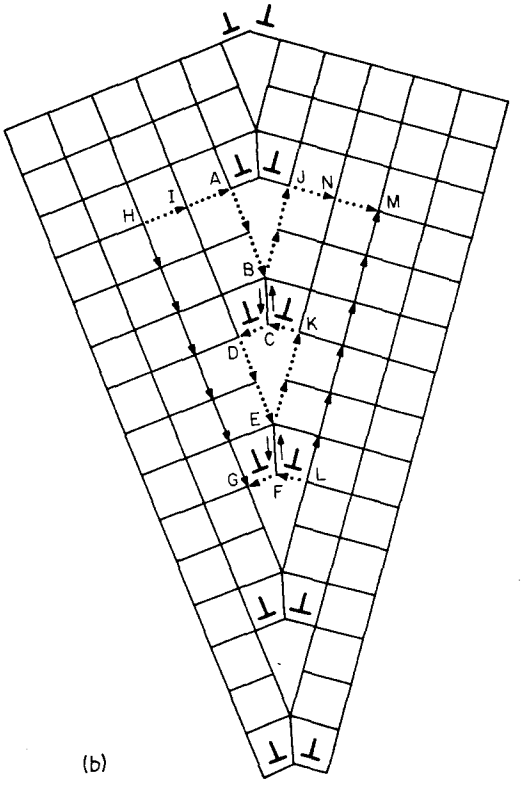

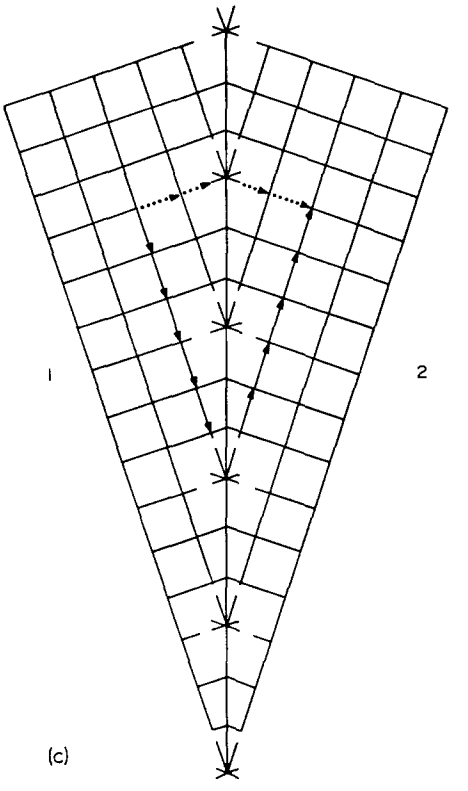

Figure 1 (a) Completely relaxed tilt-type symmetric grain boundary of misorientation angle $\theta = 36.9°$. (b) Partially coalesced modification of the grain boundary shown in (a). (c) Total coalescence of the grain boundary shown in (a).

2. Surface dislocation model of coalescence

Coalescence of the grain-boundary surfaces eliminates the surface area associated with ledge steps. The ledge steps eliminated during coalescence are converted into elastic dislocations which have stress and strain field associated with them. This very important result shows the intimate relation between the elimination of ledge steps and the formation of elastic dislocations. The coalescence in the fully torn boundaries is zero as shown in Fig. 1a and hence there are no elastic distortions and thus stress field in that boundary. The coalescence in the boundary shown in Fig. 1c is the total, thus converting the ledge step completely into an elastic dislocation. A partially coalesced boundary, as shown in Fig. 1b, has elastic dislocations and stress field associated with it.

Consider the Burgers circuit ABCDEFGHIA in the grain-boundary region shown in Fig. 1b. It is seen that the ledge steps CD and FG are

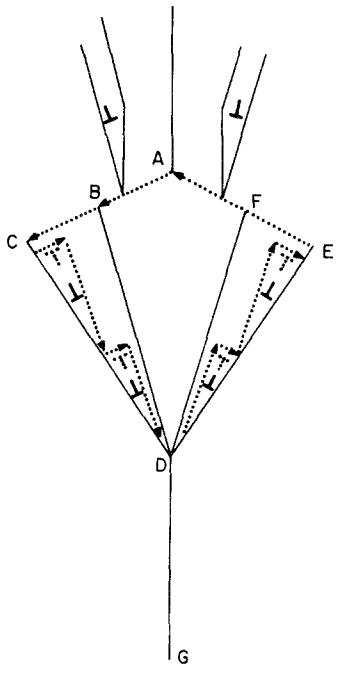

Figure 2 Enlargement of a portion of the grain boundary shown in Fig. 1b.

smaller than HI and IA, respectively, as a result of the coalescence of the grain-boundary surfaces. The grain-boundary dislocations with Burgers vector CD and FG have no stress field, but their Burgers vector is smaller than HI and IA. These grain-boundary dislocations are termed compensated dislocations. The difference between the Burgers vector of the grain-boundary lattice dislocation and the compensated dislocation constitutes the Burgers vector of the elastic dislocation formed due to coalescence. The stress field associated with the partially coalesced boundary, as pointed out before, is also due to the elastic dislocations formed. Similarly a Burgers circuit can be made in the grain on the right-hand side of Fig. 1b. It is now obvious that full coalescence can only make an elastic dislocation as large as the grain-boundary dislocation, i.e. of the same magnitude of the Burgers vector. The severe distortion resulting from coalescence does not permit full coalescence; on the other hand, the surface energy is reduced by the coalescence to the extent permitted by the distortion.

In order to further understand the coalescence in terms of the grain-boundary surface array, a grain-boundary configuration is depicted in terms of the surface array as shown in Fig. 2. The coalesced region is DG. The uncoalesced grain-

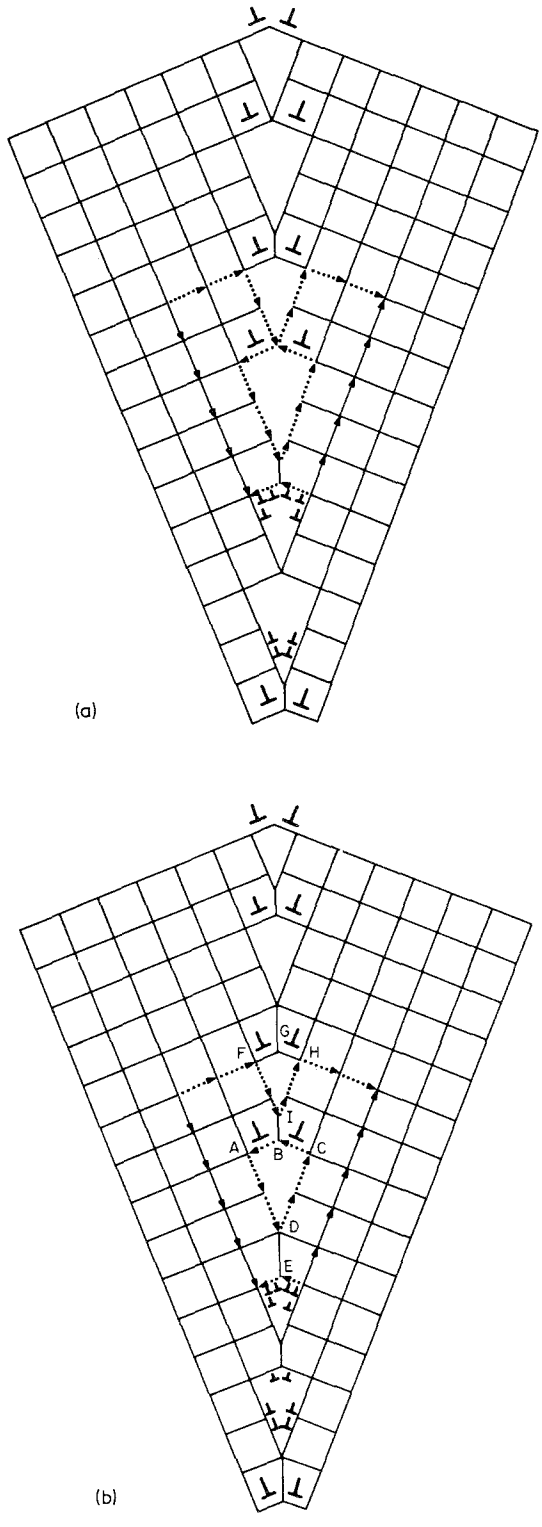

Figure 3 (a) Partial coalescence of a grain boundary consisting of non-uniform arrays of dislocations. The coalescence of the primary ledges allows the contact of the second set of ledges. (b) Further coalescence of the grain-boundary surfaces shown in (a).

boundary surfaces are ABDFA. However, in order to form the surfaces BD and DF, the elastic grain-boundary surface array is situated on the surface CD and DE. Each ledge consists of dislocations of opposite sign, one representing the ledge step shown dotted while the other shown by the full line represents the stress field. The surface dislocations on the grain-boundary surfaces bring the surface CD into coincidence with BD. During this process, the ledge step CB is converted into elastic dislocations of equal Burgers vector. Thus the sum of the Burgers vectors of the surface array is equal to BC. AB is the Burgers vector of the compensated grain-boundary dislocation.

The results illustrated above for a uniform array of grain-boundary dislocations can also be extended to a non-uniform array of grain-boundary dislocations. Fig. 3a shows a partially coalesced grain-boundary consisting of non-uniform arrays. The coalescence of the grain-boundary region allows the contact of the second set of ledges [6]. Fig. 3b shows further coalescence of the grain-boundary surfaces. It is clear from Fig. 3b that coalescence in the region BI gives rise to a secondary surface array on the surfaces FI and HI whose Burgers vector is smaller than the primary surface array on the surfaces AD and DC. Therefore, the elastic stress field in the region near D due to the primary array will be much larger than the stress field near I arising due to secondary array. The diffraction contrast must also be stronger at D than at I. Since D is only a few atoms distant, the contrast requires very high resolution experiments.

3. Screening array of dislocations

The conservation of the Burgers vector of dislocations has been used in the earlier surface dislocation models to predict the presence of a second set of surface dislocations as shown in Fig. 4. These dislocations are different from the grain-boundary array. This set of surface dislocations is termed the screening array [6–8]. This array screens the stress field around the boundary that arises due to elastic grain-boundary surface array. The position and Burgers vector of the screening array can be determined using the minimization of the total energy of the configuration. The screening array has the Burgers vectors opposite in sign and equal in magnitude to the elastic surface array on the grain-boundary surfaces. In reality, the screening array is a two-dimensional distribution around the boundary. However, in the present numerical calculations, the array will be confined to a single plane or two

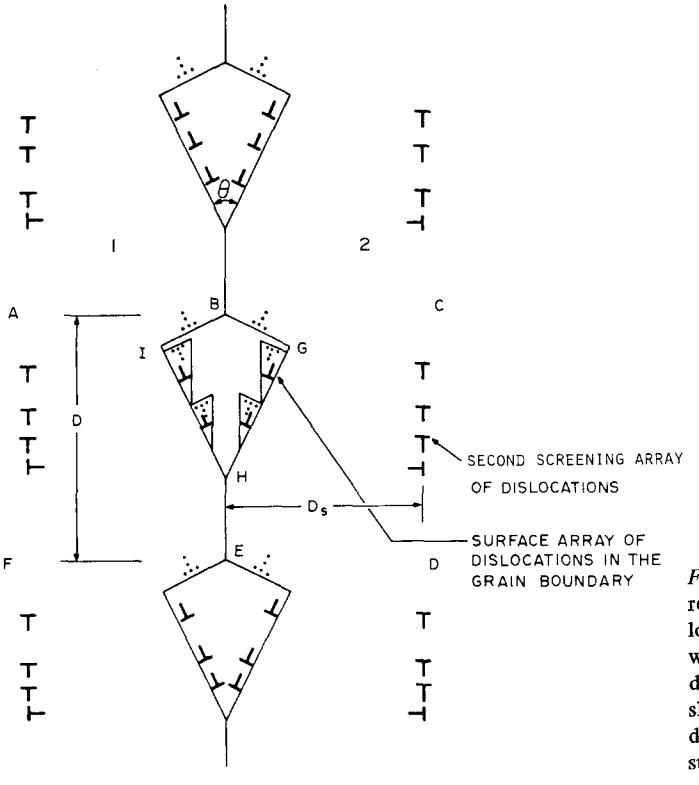

Figure 4 Three units of a grain-boundary region described in terms of the surface dislocation model. A set of surface dislocations which satisfy the free surface boundary conditions on the grain-boundary surfaces are shown together with a second set of surface dislocations which allow the screening of the stress field of the grain-boundary array.

planes in order to illustrate their effect. Physically, the array represents a relaxation of the distortion present due to the elastic grain-boundary array. Thus, the distortion spreads through space around the boundary.

The screening array exerts an attractive force on the elastic surface array, thus giving rise to an opening up effect on the grain-boundary surface. On the other hand, the grain-boundary surfaces tend to coalesce and thus reduce the surface energy. It should also be mentioned that the elastic surface dislocations repel each other; thus not allowing the grain-boundary surfaces to coalesce. The equilibrium position of the screening array depends on the balance between the increase in surface energy and the reduction in strain energy as the screening array approaches the grain-boundary surface array. The Burgers vector of the elastic surface array on the grain-boundary surfaces increases with coalescence, thus offering more opposition to coalescence. At the same time, the Burgers vector of the surface screening array also increases and exerts an opening up effect on the grain-boundary surfaces. At equilibrium, the screening array is situated at some distance from the boundary. Although the method of continuous distribution of dislocations is ideal, it is cumbersome and cannot be used for complex configurations. Therefore, the method of discrete dislocations is employed to determine the dislocation configurations using the principle of minimization of the total energy of the configuration.

4. Energy of a grain boundary using the surface dislocation model

The energy per unit length of boundary in conventional units can be computed by determining the equilibrium configuration of surface dislocations on grain-boundary surfaces as well as those required to screen the stress field, i.e. the second set of dislocations situated on planes at a distance D_s, as shown in Fig. 4. The equilibrium configuration is determined by minimizing the total energy of the configuration with respect to the position and Burgers vector of all the dislocations and the parameter, D_s. A unit of the grain-boundary region is defined for purposes of determining the energy of the configuration. The unit consists of the region ABCDEF as shown in Fig. 4. The region ABCDEF consists of the surface dislocations in region CD and AF and the elastic grain-boundary dislocation array in the partially coalesced configuration, BGHEHI. Three such units are considered in the determination of the total energy of the grain boundary. The orientation of the surface dislocations with respect to the surfaces of the grain-boundary region is shown in Fig. 4: in particular, the Burgers vector of each dislocation is perpendicular to the surfaces GH and HI and parallel to the surfaces BI and BG. The sum of the Burgers vectors of the surface dislocations on the surface BGHI should be equal to the difference between the grain-boundary lattice dislocation and the compensated grain-boundary dislocation, or equivalently, the decrease in the ledge step. The set of screening dislocations consist of those with Burgers vector perpendicular to CD and AF and parallel to these planes. The law of conservation of Burgers vectors indicates that the sum of the Burgers vectors of the set of screening dislocations with horizontal components should be equal to the sum of the horizontal components of the Burgers vector of the elastic surface array of dislocations on the grain-boundary surfaces. The vertical components of the Burgers vectors of the grain-boundary dislocations on surface GH in the configuration form a dipole with vertical components of the array on the surface HI. The second set of screening dislocations consists of those with Burgers vector parallel to the surfaces CD and AF in order to screen the σ_{xy} component of stress.

The minimum energy configuration is obtained by minimizing the total energy of the configuration as a function of position and Burgers vector of each dislocation in the configuration. In particular, the total energy of the configuration can be written as

$$E_T = E_S + E_I + E_\gamma, \qquad (1)$$

where E_S is the self energy of all the dislocations in a unit of the grain-boundary region, E_I the interaction energy of the dislocations in a unit of the grain-boundary region plus the mutual interaction energy of the dislocations with the unit above and below, and E_γ the surface energy of a unit of the uncoalesced grain-boundary surfaces. In the evaluation of the mutual interaction energy between regions above and below with the unit under consideration, only one half of the contribution should be included since this interaction is shared by two adjacent units. Expressions for the interaction energy between dislocations can be obtained from standard formulae [10]. The

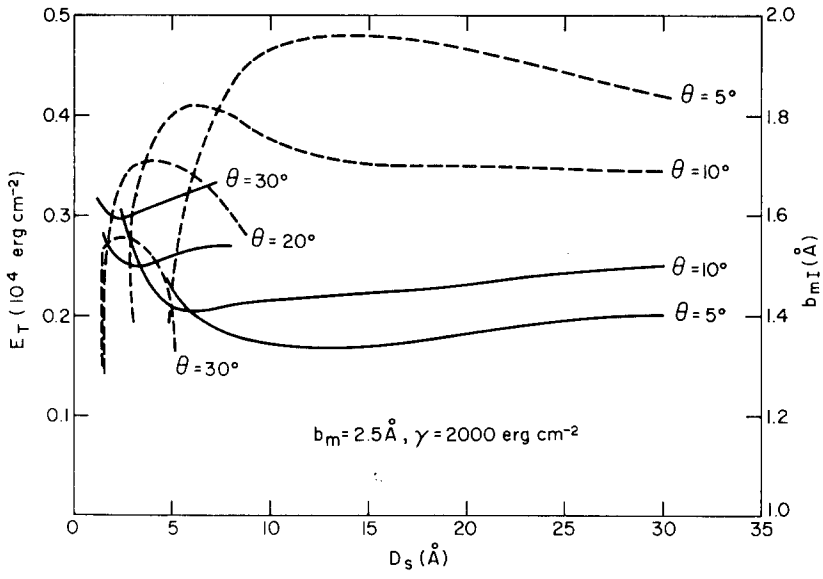

Figure 5 The total energy E_T per unit length and the sum of the Burgers vectors of the surface grain-boundary array b_{mI} shown as a function of the distance D_s. The full line curves correspond to E_T and the dashed lines to b_{mI}.

elastic constants for iron and its alloys have been used in the evaluation of the energy E_T; in particular, the shear modulus $\mu = 7.14 \times 10^{11}$ dyn cm^{-2} and Poisson's ratio $\nu = 0.3333$ have been employed. The surface energy per unit area, $\gamma = 2000$ erg cm^{-2} for iron is also assumed in the numerical calculations. Results at different values of γ are also shown. The crystal size, R, is assumed to be 1 cm. It is important at this point to note that the value of R used in the determination of the self and interaction energy terms is unimportant since the stress field of the grain-boundary array is completely screened. It can easily be shown that the energy of a dislocation configuration consisting of equal numbers of positive and negative dislocations is independent of R and depends only on the spacing between the dislocations. It is important to indicate that the angle of misorientation across the boundary-free surface is maintained constant throughout the minimization procedure so that the dislocation configuration can be determined without ambiguity. The surface dislocations on the grain-boundary surfaces GH and HI are allowed to approach one another to a distance equal to the sum of their Burgers vectors, and below this value of separation, the surfaces are considered to be coalesced at the lower end of the region BGHI; namely at point H. The total Burgers vector of the surface array on the grain-boundary surfaces is proportional to the coalesced region of the boundary. The equilibrium configuration corresponds to the minimum energy position of D_s. The energy of the configuration, E_T increases with D_s at values of D_s above that corresponding to the minimum energy position. Therefore, the screening effect of the stress field by the screening array is absent at distances above that corresponding to the minimum energy. The minimum energy configuration corresponds to the equilibrium configuration in an infinite body. Fig. 5 shows E_T as a function of D_s for different angles of misorientation, θ. Also shown in Fig. 5 is the sum of the Burgers vectors of the elastic surface dislocations on the grain-boundary surfaces. The significance of the E_T versus D_s curve for D_s less than that corresponding to the minimum energy configuration can be understood by considering the grain boundary in a finite crystal of size, D_s. The crystal size is now independent of the grain-boundary configuration and the second set of screening dislocations satisfy the free surface boundary conditions on the surfaces of the finite crystal. The value of E_T increases with decreasing size of the crystal, D_s since the surface dislocation arrays on the surfaces of the finite crystal attract the surface array on the grain-boundary surfaces and thus tend to increase the grain-boundary surface area. The sum of the Burgers vectors of the surface array on the grain-boundary surfaces is found to reach a maximum at the minimum energy configuration. The coalescence of the grain-boundary surfaces reaches a maximum at the minimum energy con-

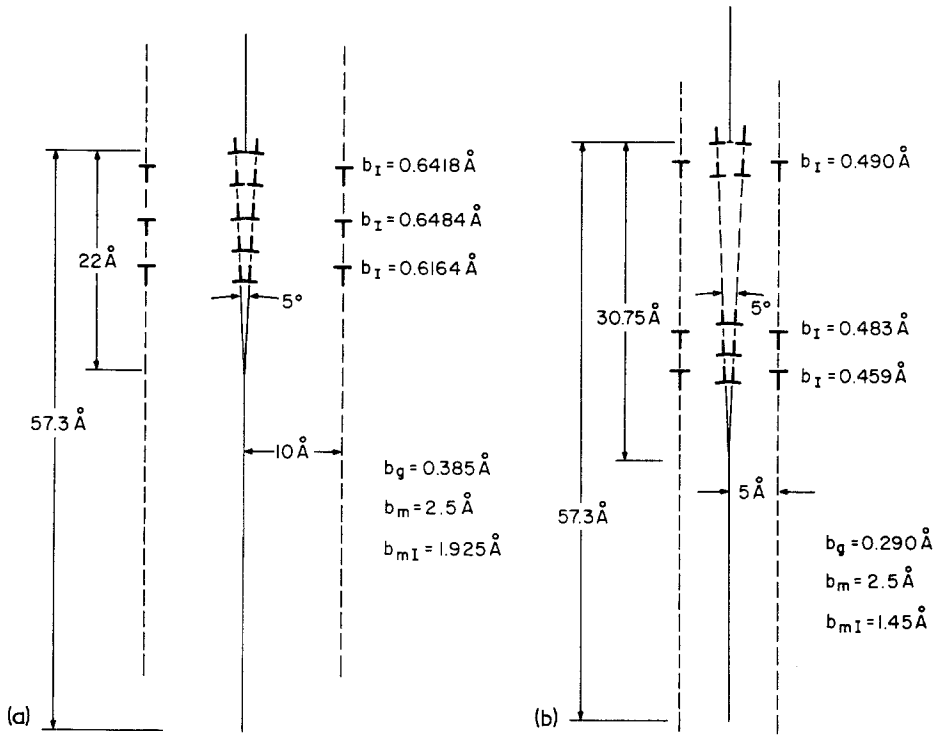

Figure 6 (a) The dislocation configuration of a partially coalesced grain boundary of misorientation angle $\theta = 5°$. The Burgers vector of the dislocation in the surface array, $\boldsymbol{b}_g$, the Burgers vector of the grain-boundary lattice dislocation, $\boldsymbol{b}_m$, the Burgers vector of the screening array, $\boldsymbol{b}_I$ and the sum of the Burgers vectors of the screening array $\boldsymbol{b}_{mI}$ are all shown. The equilibrium distance D_s is 10 Å. (b) As (a) but with D_s smaller than the equilibrium value.

figuration giving the maximum Burgers vector of the elastic surface array of dislocations on the grain-boundary surfaces. Also, when the grain-boundary surfaces open up, the Burgers vector of the surface array decreases. The value of E_T at the minimum energy is found to increase with increasing values of θ. On the other hand, the sum of the Burgers vector of the surface array decreases with increasing θ. Thus the elastic dislocation content of a boundary decreases with increasing θ, finally becoming zero at $\theta = \pi/2$. This result is in agreement with the general belief that high-angle boundaries have smaller elastic distortions associated with them and thus smaller elastic dislocation contents.

Fig. 6a shows the dislocation configuration of the grain boundary in an infinite crystal together with the second set of screening dislocations. The surface array on the surfaces CD and AF for $\theta = 5°$ have Burgers vectors with horizontal component only. The surface array is also uniformly distributed. When the size of the crystal is reduced, the dislocation configuration for $\theta = 5°$ is shown in Fig. 6b. The grain-boundary surfaces have separated further and the screening array is also not uniform. The arrangement of dislocations above the coalesced region is a measure of the distortion present. Fig. 7a shows the dislocation configuration with minimum energy for $\theta = 10°$. The screening array of dislocations have Burgers vectors, both perpendicular and parallel to the grain-boundary surface. When the size of the crystal is reduced for $\theta = 10°$, the configuration shown in Fig. 7b obtains. The grain-boundary array and the screening array are non-uniform. The arrangement of dislocations above the coalesced region shows the nature of the distortion. The dislocation configurations at the minimum energy for $\theta = 20°$ and $30°$ are shown in Fig. 8a and b, respectively. The Burgers vectors of the dislocations are also shown in the figures. These configurations at the equilibrium spacing of D_s indicate that the set of screening dislocations with a horizontal component remain almost uniformly spaced for all values of θ. The results also show that the conservation of Burgers vectors is satisfied within the accuracy of the discrete dislocation analysis. The total energy of the grain-boundary per unit length

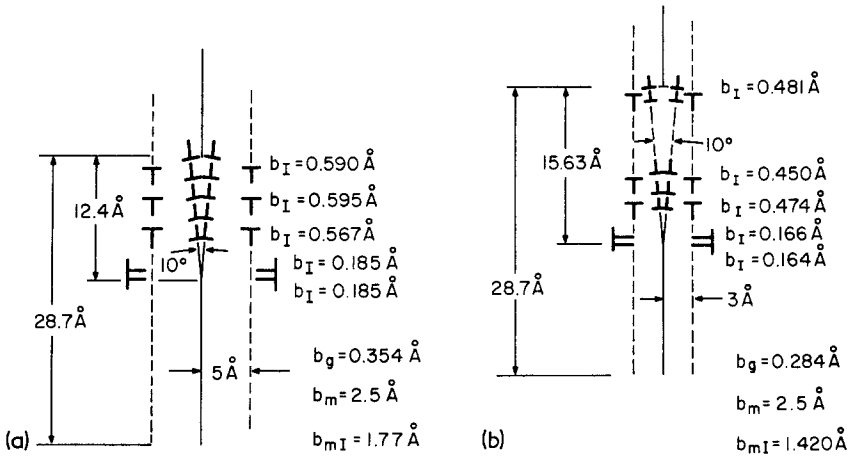

Figure 7 (a) As Fig. 6a but with $\theta = 10°$. (b) As Fig. 6b but with $\theta = 10°$.

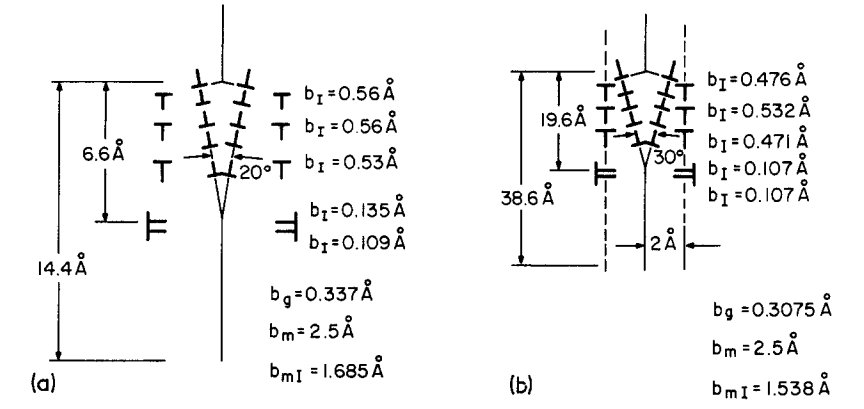

Figure 8 (a) As Figs. 6a and 7a but with $\theta = 20°$. (b) As Figs. 6a, 7a and 8a but with $\theta = 30°$.

is shown in Fig. 9. The results show the absence of a maximum in the energy as a function of θ. Also, when γ is decreased to 500 erg cm^{-2}, the energy values are decreased by more than half. The value of the surface energy of the grain-boundary surfaces is not known exactly. Since the grain boundary surfaces are separated by only a few atomic distances, the surface energy cannot really possess its free surface energy value, γ. In addition, the separation between the grain-

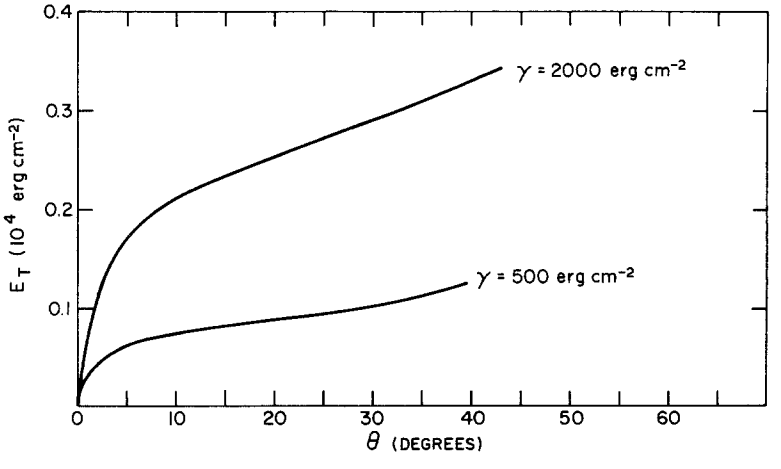

Figure 9 The energy of the grain boundary per unit length shown as a function of θ for two values of surface energy.

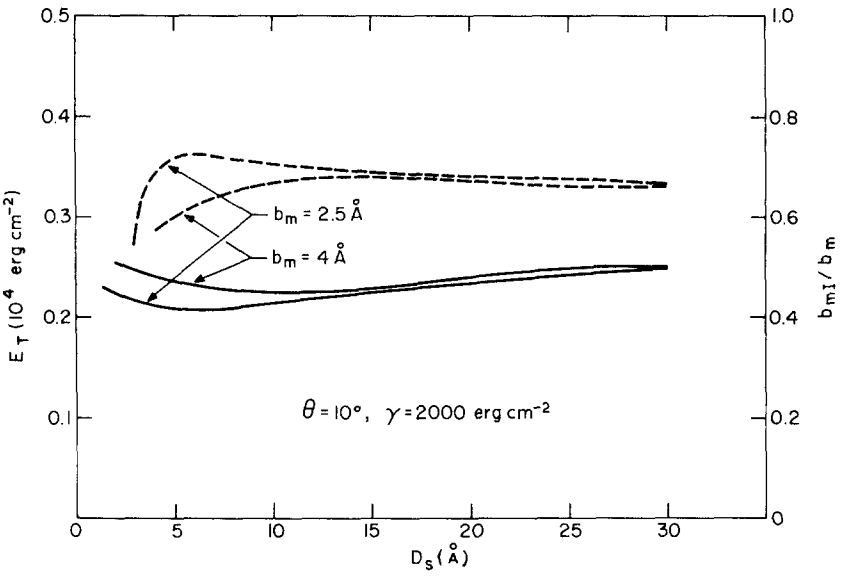

Figure 10 Energy per unit length of the grain boundary E_T and the sum of the Burgers vectors of the grain-boundary surface array, b_{mI} as a function of D_s for $\theta = 10°$. E_T is shown by full lines and b_{mI}/b_m shown by dashed lines. The results are illustrated for two values of the Burgers vector of the grain-boundary lattice dislocation, b_m.

boundary surfaces changes from one atomic distance at the coalesced region to a few atomic distances at the top. Therefore, while the energy versus θ curve is qualitatively correct, the exact result depends on the determination of the surface energy as a function of distance of separation of the grain-boundary surfaces. The absence of cusps in Fig. 9 is not unexpected since the grain-boundary energy is determined at values θ equal to 5, 10, 20, 30 and 40 degrees which do not include the coincidence orientations. If the calculations are performed incorporating the exact crystallography of the boundary, minimum energy configurations are expected to show up in the energy versus θ curve.

It is useful to consider a grain boundary with the Burgers vector of the grain-boundary lattice dislocation subdivided without altering the grain-boundary misorientation angle. Subdividing the grain-boundary ledges *ad infinitum* leads to a boundary with zero energy, i.e. two grains of proper orientation are joined together without the necessity of any dislocations to account for the misorientation. The result of subdividing the boundary on the energy of the boundary is shown in Fig. 10. When the Burgers vector of the lattice dislocation, b_m comprising the boundary is reduced from 4 Å to 2.5 Å, the minimum in the energy is shifted from $D_s = 10$ Å to $D_s = 5$ Å. This result obtained for $\theta = 10°$ will be different quantitatively at the other values of θ. Similarly, the sum of the Burgers vector of the surface array of elastic dislocations on the grain-boundary surfaces, b_{mI} increases with decreasing Burgers vector of the lattice dislocation, b_m. When the Burgers vector is infinitesimally small, the minimum energy configuration is siatuated at the origin, i.e. D_s at equilibrium is zero.

The necessity of the screening array of dislocations has been justified by the presence of a minimum energy as a function of distance of separation from the boundary. Previously, it has been pointed out that the screening array is in general a two-dimensional distribution. In order to verify the nature of the distribution of the screening array two sets of screening dislocation arrays are considered at distances D_{s_1} and D_{s_2} from the boundary on either side as shown in Fig. 11. The screening array of dislocations with Burgers vector perpendicular to the grain boundary only is considered in the analysis. The total energy of the configuration is minimized with respect to the position and Burgers vector of all the surface dislocations and also with respect to D_{s_1} and D_{s_2}. The total energy of the configuration E_T as a function of D_{s_2} for three values of D_{s_1} is shown in Fig. 12. It is seen that for $D_{s_2} > D_{s_1}$, E_T reaches a minimum as a function of D_{s_2} for a given value of D_{s_1}. Also, the minimum value of E_T at $D_{s_1} = 5$ Å and $D_{s_2} = 10$ Å has been found

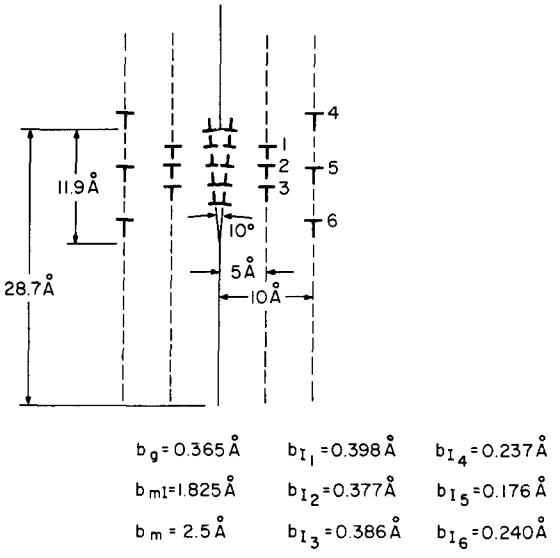

Figure 11 The dislocation configuration of a grain boundary of misorientation angle $\theta = 10°$ with two sets of screening arrays of dislocations shown at equilibrium. The Burgers vectors of all the surface dislocations are shown in the figure.

to correspond to equilibrium for the grain boundary with misorientation angle $\theta = 10°$. Fig. 12 also shows the sum of the Burgers vector of the surface array of dislocations $\boldsymbol{b}_{mI}$ as a function of D_{s_2} for three values of D_{s_1}. The maximum of $\boldsymbol{b}_{mI}$ at $D_{s_1} = 5$ Å and $D_{s_2} = 10$ Å corresponds to the maximum coalescence of the grain-boundary surfaces at equilibrium. The dislocation configuration shown in Fig. 11 with $D_{s_1} = 5$ Å and $D_{s_2} = 10$ Å proves that the conservation of Burgers vectors is satisfied within the accuracy of the discrete dislocation analysis. The Burgers vector of the screening array at $D_{s_1} = 5$ Å is larger than the Burgers vector of the screening array at $D_{s_2} = 10$ Å. The stress field and distortion around the boundary decreases at larger distances from the boundary and hence the Burgers vector of the screening array also decreases. The screening array at D_{s_2} also spreads to larger distances showing the spreading of the distortion around the boundary. The presence of a minimum in energy as a function of both D_{s_1} and D_{s_2} once again proves the result that the distribution of screening array of dislocations is in fact two-dimensional. It is important to note that while the stress field of the surface array of the grain-boundary dislocations is concentrated in the grain-boundary region, the distortion around the boundary is spread out. Thus, the diffraction contrast of the screening array around the grain boundary is not sharp but it is expected to give a general background effect. Finally, Fig. 13a and b show a favourable rearrangement of grain-boundary lattice dislocations which is also equal to translating the fully torn boundaries before coalescing them [3]. This modification however,

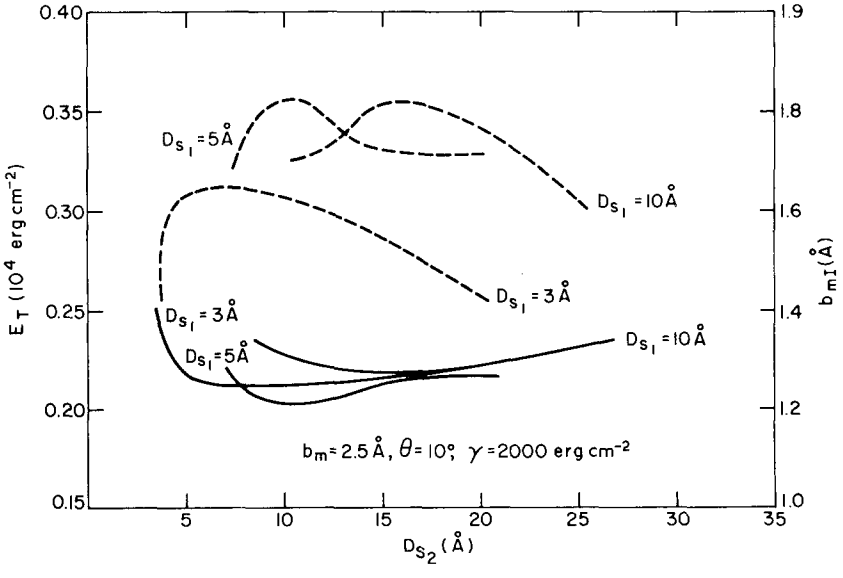

Figure 12 The total energy per unit length, E_T and the sum of the Burgers vectors of the surface array of dislocations on the grain-boundary surfaces, $\boldsymbol{b}_{mI}$ shown as a function of D_{s_2} for three values of D_{s_1}. D_{s_1} and D_{s_2} are the distances of the screening arrays from the grain boundary. E_T is shown by full lines while $\boldsymbol{b}_{mI}$ is shown by dashed lines.

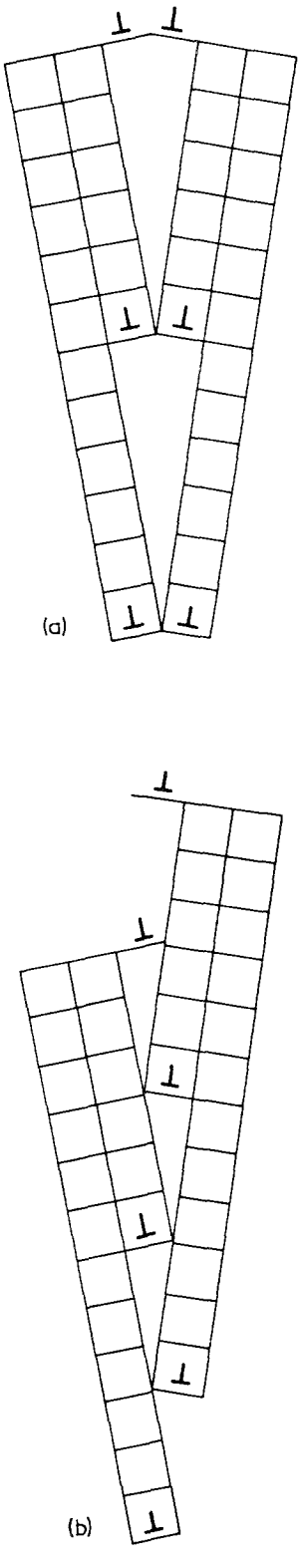

Figure 13 (a) Completely relaxed low-angle boundary of misorientation $\theta = 18.9°$. (b) Dissociated modification of the grain boundary shown in (a).

does not significantly alter the concepts associated with the fine structure of grain boundaries as already considered [5, 8] and the extension of those ideas to Fig. 13a and b is rather straightforward.

5. Significance of results obtained using the surface dislocation model

In the present refined surface dislocation model of a grain boundary of any angle of misorientation, the continuum model is developed to account for the property of surfaces to coalesce and thus reduce the energy of the configuration. The present surface dislocation model also shows that the elastic dislocation content of a boundary depends on the degree of coalescence of the boundary surfaces. The elastic dislocation content of the boundary decreases with increasing angle of misorientation since the coalescence of the boundary surfaces decreases. The nature of distribution of surface dislocations on the grain-boundary surfaces correctly illustrates the regions where the distortion is severe, namely those regions where coalescence takes place to the largest extent. The high dislocation density at the tip regions of the partially coalesced grain boundary could also explain the non-linear nature of the distortion.

The surface dislocation model of the grain boundary obtained here can be used to explain the diffraction contrast, say as obtained in the electron microscope. The stress field and the distortion present in the boundary is very easily predicted from the coalesced grain-boundary configurations and thus the diffraction contrast obtained from the dislocation configurations.

6. Conclusions

The surface dislocation analysis of a grain boundary of any misorientation angle is carried out taking into account the tendency of the grain-boundary surfaces to coalesce in order to reduce the surface energy. In this refined model, the elastic dislocation content of the boundary is shown to be proportional to the degree of coalescence of the boundary. The elastic dislocations are created as a result of the elimination of the ledge steps. The Burgers vector of the elastic dislocations on the grain-boundary surfaces is equal to the magnitude of the ledge step eliminated. The principle of conservation of Burgers vectors is used to predict the presence of a screening array of dislocations. The position of the screening

array from the grain-boundary array is determined by the balance between the surface energy of the grain-boundary surfaces and the strain energy of the dislocation configuration. The screening array represents the relaxation of the distortion present around the boundary. The screening array is in general a two-dimensional distribution in the medium surrounding the boundary. This result has been verified by the presence of a minimum energy configuration containing two arrays of screening dislocations situated at different distances from the boundary. The dislocation configuration in the coalesced regions of the boundary is an indication of the distortion and stress field in the boundary. The diffraction contrast due to the surface array of dislocations on the grain-boundary surfaces can be inferred from the arrangement of surface dislocations. The distortion due to the screening array of dislocations cannot give rise to a sharp diffraction contrast but represents instead a general background. The discrete dislocation analysis employed in conjunction with the surface dislocation model of the grain boundary correctly describes the structure of the grain boundary and the coalescence of the grain-boundary surfaces. The elastic dislocation content of the boundary has been found to decrease with increasing misorientation angle.

Acknowledgements

The computer time for the present investigation was provided in full through the facilities of the Computer Science Center of the University of Maryland. Financial support for the present study was provided by the US Department of Energy under contract no. AT-(40-1)-3935.

References

1. M. J. MARCINKOWSKI, K. SADANANDA and W. F. TSENG, *Phys. Stat. Sol. (a)* **17** (1973) 423.
2. M. J. MARCINKOWSKI and K. SADANANDA, *ibid.* **18** (1973) 36.
3. K. SADANANDA and M. J. MARCINKOWSKI, *J. Appl. Phys.* **45** (1974) 1521, 1533.
4. M. J. MARCINKOWSKI and K. SADANANDA, *Acta Crystallogr.* **A31** (1975) 280.
5. W. BOLLMAN, "Crystal Defects and Crystalline Interfaces" (Springer-Verlag, Berlin, 1970).
6. M. J. MARCINKOWSKI and K. JAGANNADHAM, *Phys. Stat. Sol. (a)* **50** (1978) 293.
7. K. JAGANNADHAM and M. J. MARCINKOWSKI, *ibid.* **50** (1978) 601.
8. *Idem, Crystal Lattice Defects* 8 (1979) 81.
9. M. J. MARCINKOWSKI, "Unified Theory of Mechanical Behaviour of Solids" (Wiley, New York, 1979).
10. J. P. HIRTH and J. LOTHE, "Theory of Dislocations" (McGraw Hill, New York, 1968).

Received 10 April and accepted 19 July 1979.